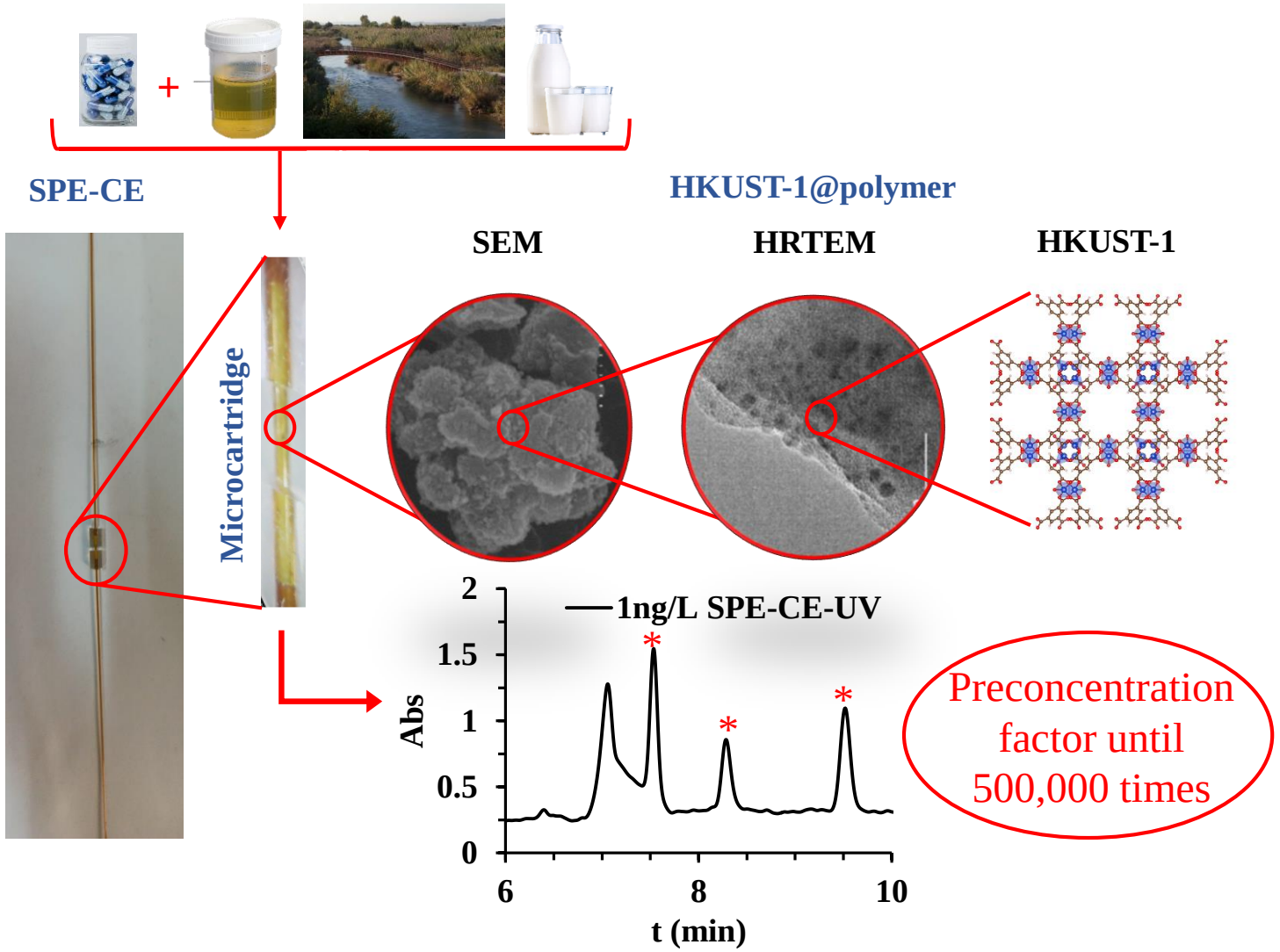

Graphical abstract Martínez-Pérez-Cejuela et al.

Highlights

- A HKUST-1@polymer was applied for the first time as sorbent for SPE-CE-UV.
- A nano-MOF was built layer-by-layer onto a polymer and further characterized.
- Up to 500,000 times sensitivity enhancement compared to CE-UV was achieved.
- Fluoroquinolones were analyzed in environmental, food and biological samples.

A hybrid nano-MOF/polymer material for trace analysis of drugs in complex matrices at microscale by on-line solid-phase extraction capillary electrophoresis with UV detection

Héctor Martínez-Pérez-Cejuela[1], Fernando Benavente[2]*, Ernesto F. Simó-Alfonso[1], José Manuel Herrero-Martínez[1]*

[1]*Department of Analytical Chemistry, University of Valencia, c/Dr. Moliner, 50, 46100-Burjassot, Valencia (Spain).*

[2]*Department of Chemical Engineering and Analytical Chemistry, Institute for Research on Nutrition and Food Safety (INSA·UB), University of Barcelona, Barcelona, Spain*

*Prof. José Manuel Herrero-Martínez, e-mail: jmherrer@uv.es; Tel: +34963544062; Fax: +34963544436

*Prof. Fernando Benavente, e-mail fbenavente@ub.edu; Tel: +34934035423; Fax: +34934021233

ORCID numbers:

Héctor Martínez Pérez-Cejuela: 0000-0002-6456-0846

Fernando Benavente: 0000-0002-1688-1477

Ernesto F. Simó-Alfonso: 0000-0001-7502-6350

José Manuel Herrero-Martínez: 0000-0002-8745-3795

Abstract

A hybrid composite (nano-metal organic framework@organic polymer, named as nano-MOF@polymer) was applied for the first time as sorbent for on-line solid-phase extraction capillary electrophoresis with ultraviolet detection (SPE-CE-UV). The composite was prepared building layer-by-layer a HKUST-1 (Hong Kong University of Science and Technology-1) nano-MOF onto the polymer surface, which allowed controlling the thickness and maximizing the active surface area. The sorbent was widely characterized at micro- and nano-scale to validate the synthesis and to establish the material properties. Then, fritless microcartridges (2 mm) were assembled by packing only a few micrograms of sorbent particles and investigated for preconcentration of fluoroquinolones (FQs) in several real samples (river water, human urine and whole cow milk). Under the optimized conditions, the sample (*ca.* 60 µL) was loaded in separation background electrolyte (BGE, 50 mM phosphate (pH 7)), and retained analytes were eluted using a small volume of 2% v/v formic acid in methanol (*ca.* 50 nL). The SPE-CE-UV method was validated in terms of linearity, limit of detection (LOD), limit of quantification (LOQ), repeatability, reproducibility and reusability. The developed method showed a LOD decreasing until 1 ng L^{-1} when larger volumes of sample were loaded (*ca.* 180 µL), which was 500,000 times lower than by CE-UV. This undescribed sensitivity enhancement would arise from the homogenous and populated MOF nano-domains and the appropriate permeability of the composite, which would promote high extraction efficiency and loading capacity. Furthermore, the sorbent showed appropriate selectivity regardless the analyzed complex environmental, biological or food matrix samples, achieving excellent detectability and recoveries (> 90%).

Keywords: capillary electrophoresis, fluoroquinolones, hybrid composite, metal organic framework, on-line solid-phase extraction, microscale

1. Introduction

Metal-organic frameworks (MOFs) are coordination polymers built from suitable organic ligands and metal ions that form ordered porous networks [1]. They present several fascinating properties for analytical chemistry [2] and other research fields such as large surface area, chemical stability, tunable chemistry, etc., which have been demonstrated over the years [3,4].

Nowadays, nanoscale materials are of great interest for a large variety of applications [5,6]. New or improved features appear when material size is reduced. In particular, regarding nano-MOFs, an enlarged surface area and superior mass transference (due to the short transport routes) lead to a major accessibility of the active sites for the target analytes [7,8].

Several approaches can be followed to decrease and control the particle size of MOFs, such as assisting the synthesis with ultrasound [7,9] or introducing modulators in the precursor mixtures [10,11]. Alternatively, the layer-by-layer assembly [12–14] allows controlling not only the particle size, but also maximizing the active surface area for analyte interaction [15]. In addition, the MOF layers can be built up in a polymeric organic support to obtain a hybrid composite [12,16] with superior features than the individual components. As unique advantage, the layer-by-layer approach does not require high temperature/pressure neither toxic solvents (e.g. solvothermal or reflux) [17], and preparation times can be shorter if the number of synthetic cycles are restrained.

To date, the potential of nano-MOF composites has been explored in gas storage [18], as carrier platform [19], sensing [20], catalysis [21] and separation [22], among other fields. Meanwhile, the investigation of nano-MOFs in sample treatment is still in its first steps, especially at the microscale application [2]. Several challenges remain in the design of nano-MOF based composites as sorbents for the efficient sample clean-up and

preconcentration when dealing with samples of limited volume and miniaturized techniques [16]. In this regard, on-line solid-phase extraction capillary electrophoresis (SPE-CE), which requires minute amounts of such sorbents, is an excellent candidate to demonstrate and expand the applicability in microextraction of nano-MOFs and their hydrid polymeric composites [23–29].

In SPE-CE [25–29], a microcartridge containing an appropriate sorbent is connected near the inlet of the separation capillary. The microextraction device allows loading a larger volume of sample than in conventional CE (hundreds of μL vs tens of nL), retaining the analytes of interest and cleaning-up the sample matrix interferences. The analyte preconcentration is achieved after injecting a small volume of eluent (tens of nL) before applying the voltage for the separation and detection. Nowadays, SPE-CE is widely recognized as an efficient and versatile strategy to enhance sensitivity of CE, obtaining typical preconcentration factors from 100 to 10,000 [25]. A broad range of sorbents with different selectivity have been applied to analyze a great variety of analytes, from commercial chromatographic particle sorbents [25] (C8, C18, HLB, cationic or anionic exchange, etc.) to less conventional particle sorbents based on immunoaffinity [26], silicon carbide [27], aptamer affinity [28] and polymeric monoliths with gold nanoparticles [29]. In all cases, as with many other extraction techniques at the microscale that require a minute amount of sorbent, SPE-CE struggles with the necessity of improving extraction efficiency and loading capacity, while decreasing non-specific retention. In addition, in SPE-CE is also crucial to make compatible the sorbent physicochemical characteristics and retention/elution mechanisms with the on-line electrophoretic separation and detection. Therefore, the development of novel high-performance sorbents to further expand the applicability of microextraction techniques, including SPE-CE, is a major concern.

In this study, a hybrid composite made up of a nano-MOF (HKUST-1, Hong Kong University of Science and Technology-1) and an organic polymer (synthesized with methacrylic acid (MAA) as monomer) was prepared, characterized and applied as sorbent in SPE-CE with ultraviolet detection (SPE-CE-UV). The method was optimized and validated with standards and then applied to river water, human urine and whole cow milk samples. The nano-MOF was built onto the monolithic polymer using the layer-by-layer approach. The resulting material was extensively characterized at micro- and nano-scale, before investigating its applicability for the trace analysis of drugs in complex samples. Fluoroquinolones (FQs), which are a widely used group of broad-spectrum antibiotics in human and veterinary medicine, were selected as target compounds. Due to their extensive use, they have a great interest in pharmaceutical, environmental and food analysis. As far as we know, this is the first study reporting a nano-MOF@polymer composite as sorbent for SPE-CE.

2. Experimental section

Reagents, materials, sample collection, instruments and apparatus are included in the electronic supplementary information.

2.1. Synthesis of organic polymer

The porous polymer monolith was prepared according to a previous study with minor changes [12]. Briefly, the functional monomer and the cross-linker were MAA (liquid, 0.0435 g) and EDMA (liquid, 0.4628 g), respectively. Porogenic solvents were DMSO (liquid, 1.5005 g) and PEG-6000 (solid, 0.4981 g). A pre-polymerization mixture was weighed in a glass vial and heated (60 ºC) to dissolve the PEG. Then, after reaching room temperature, the initiator AIBN (0.0049 g) was added and homogenized using a vortex,

sonicated for 15 min in an ice bath (to avoid heat up during sonication), and purged with a nitrogen stream for 10 min before carrying the polymerization in an oven (60 ºC) overnight. After this time, the monolith was cooled at room temperature and the bulk material was milled with a ceramic mortar. The powder was washed with MeOH several times to remove unreacted reagents and dried under vacuum. Finally, it was sieved and particles ranging in size from 100 to 200 μm were selected for nano-MOF layer-by-layer preparation.

2.2. Growth of HKUST-1 onto polymer surface

Layer-by-layer assembly was the approach selected to build the hybrid composite [12]. Concisely, two solutions were prepared: solution a) containing 10 mmol (199.2 mg) of $Cu(AcO)_2 \cdot H_2O$ in 100 mL of EtOH; and solution b) containing 10 mmol (209.5 mg) of H_3BTC in 100 mL of EtOH. Both were sonicated until homogenization. After that, 250 mg of organic polymer powder was weighed in a polypropylene tube and 10 mL of solution a) was added and magnetically stirred for 15 min. After washing with EtOH, 10 mL of solution b) was dropwise added under magnetic stirring and then the stirring was kept for 30 more minutes. Then, the material was washed again with EtOH to complete a MOF layer. The synthesis was finished after completing 4 cycles, as in our previous study [12]. The resultant blue powder was collected by vacuum filtration (nylon filter, 0.22 μm pore diameter) and gently rinsed with MeOH. The composite was air dried under vacuum at room temperature and sieved to save particles with size higher than 200 μm.

The material synthesis was thoroughly monitored by measuring the absorbance of the supernatant of solutions a) and b) before and after each impregnation step at the absorption maxima of both reagents (800 nm for Cu(II) acetate and 252 nm for organic linker).

2.3. CE

CE-UV experiments were done at 25 ºC in a 57 cm total length (L_T) (48.5 cm effective length, L_D) × 75 µm internal diameter (i.d.) × 375 µm outer diameter (o.d.) capillary. New capillaries were activated flushing at 930 mbar with H_2O (15 min), 1 M NaOH (15 min) and H_2O (15 min). Between analyses, the same sequence of solutions was used for conditioning but reducing the step durations to 2 min. Between days, capillaries were regenerated flushing with 1 M HCl (15 min) followed by the activation sequence. Samples were injected at 50 mbar for 3 s (*ca.* 35 nL, calculated with the Hagen-Poiseuille equation [30]). The separation voltage was +20 kV (cathode in the outlet end, normal polarity) and the detection wavelength was 280 nm. If necessary, capillaries were stored for short periods of time (1-5 days) after flushing with water for 2 min. For long-term storage, the capillaries were dried with air.

The optimized BGE was a 50 mM phosphate buffer solution at pH 7. It was prepared daily weighing Na_2HPO_4 (397 mg) and NaH_2PO_4 (303 mg) in a polypropylene tube. Next, 80 mL of water was added and properly mixed. Then, the pH was adjusted to 7 using 0.1 M NaOH. Finally, the solution volume was made up to 100 mL in a volumetric flask. The BGE was degassed for 15 min by sonication before its use. The 2 M phosphate buffer solution for sample preparation was prepared following the above-mentioned protocol with minor modifications.

2.4. SPE-CE

Figure S1 shows a picture of a SPE-CE capillary installed in the cartridge cassette with the microcartridge inserted near the inlet end, and some magnifications under the microscope. Fritless particle-packed microcartridges were prepared as described elsewhere with some modifications [25]. In order to avoid excessive backpressure,

capillary blockage and electric current failure during SPE-CE experiments, it was necessary to pack the microcartridges with a very small amount (2 mm length, *ca* 100 µg) of 200-250 µm nano-MOF@polymer particles. The use of sorbent particles with a size larger than the inner diameter of the separation capillary (75 µm) made unnecessary frits to avoid particle leaking during the operation. The microcartridge body (4 mm L_T × 250 µm i.d. × 375 µm o.d.) was half-full filled by vacuum with the sorbent particles, while the inlet fragment of the separation capillary (8.3 cm L_T × 75 µm i.d. × 375 µm o.d.) was connected to one of the ends with a plastic sleeve. Then, the SPE-CE capillary was extended to full length connecting to the other end the outlet fragment of the separation capillary (48.3 cm L_T × 75 µm i.d. × 375 µm o.d.). In order to ensure mechanical resistance and to extend the operation even flushing at 2 bar, the microcartridge was sealed forming a capsule with a bi-component epoxy-resin glue (Figure S1A).

Under the optimized conditions, SPE-CE capillaries were conditioned by flushing at 930 mbar with H_2O (5 min), MeOH (10 min) and BGE (5 min), followed by application of 20 kV voltage and a final flush with water (15 min). After this packing conditioning step, the volume collected by flushing water at 930 mbar for 10 min was *ca.* 60 µL. The capillary was discarded if collected volumes were significantly different than this value. Standard and sample solutions were loaded at 930 mbar for 10 min. Then, the capillary was washed by flushing with BGE for 60 s to eliminate interferences and fill the capillary before the separation. The retained analytes were eluted at 100 mbar for 5 s with a small volume (*ca.* 50 nL) of 2% FA (formic acid) v/v in MeOH. The plug of eluent was pushed from the inlet with BGE at 100 mbar for 60 s to improve repeatability between analyses and to avoid current disruption or failure. Finally, +20 kV were applied for the electrophoretic separation at 25 ºC. To avoid carry over between consecutive analyses, the capillary was flushed with MeOH (90 s) and H_2O (60 s).

2.5. Quality parameters

The quality parameters for SPE-CE were determined with standard mixtures as follows: linearity was investigated at concentrations ranging from 0.1 to 80 µg L^{-1}; repeatability (intra-day, single microcartridge and n=5) and reproducibility (inter-day, 3 days, single microcartridge/day and n=5) were evaluated at 1 µg L^{-1} as the relative standard deviation (%, RSD) of peak areas. The LOD and limit of quantification (LOQ) were determined from the most diluted analyzed mixture when S/N values were 3 or 10, respectively. The reusability was evaluated by consecutive analyses at 1 µg L^{-1}. The microcartridge was discarded when the peak areas decreased more than 20% compared to the mean value of the first three analyses with the microcartridge under consideration.

2.6. Sample analysis

The samples of river water and urine were firstly tempered and an appropriate volume of 2 M phosphate solution was added to obtain a final concentration of 50 mM phosphate in the loading samples. Then, pH was adjusted to 7 with 0.1 M NaOH. The mixtures were shaken and left 30 min in the darkness. After this period, they were centrifuged for 15 min at 4,500 g and vacuum filtered (nylon filter, 0.22 µm pore size) to remove suspended matter. For urine sample, a 1/10 dilution was made before the SPE-CE analysis due to the complexity of the matrix. Fortified samples (1 µg L^{-1}) were prepared by spiking the river water and urine samples before the sample preparation with appropriates volumes of FQ standard mixture (100 mg L^{-1}).

In the case of whole cow milk, the samples were tempered and protein precipitation was accomplished by mixing cold MeCN (stored at -20 ºC) with milk samples at a 6:1 ratio (v/v). Then, the mixture was vortexed for 90 s and kept in the freezer for 1 h to ensure the maximum protein precipitation. After that, the suspension was centrifuged for 15 min at

4,500 g. The supernatant was collected and the remaining pellet was rinsed twice with cold MeCN (*ca.* 1/10 of the ACN volume used in the precipitation step). After agitation and centrifugation, supernatants were pooled and evaporated to dryness using miVAC sample concentrator (centrifugation at 25 ºC under vacuum). Finally, the samples were reconstituted to the original volume with BGE and the pH was readjusted to 7 with 0.1 M HCl before SPE-CE analysis. Fortified milk samples (1 μg L^{-1}) were prepared as for river water and urine samples.

3. Results and discussion

3.1. Choice of material

The selection of the right material in SPE is critical since it will strongly influence recoveries, and subsequently, method performance. The nano-MOF@polymer composite was designed taking advantage of the monolithic features (good permeability, cheap and simple synthesis) [29,31,32] and the MOF characteristics (great surface area, selectivity, high surface-to-volume ratio, among others) [2,13]. Thanks to that, the resulting sorbent will overcome typical problems encountered with other sorbents such as limited recoveries, inappropriate particle size, heterogeneity, losses of material or high backpressures [16,33]. The composite was prepared using the layer-by-layer approach since it allows a reproducible synthesis controlling the thickness and maximizing the active surface area [34,35]. A MAA based monolith was selected since it presents a great number of carboxylic residues for Cu(II) coordination. The specific choice of HKUST-1 against the existing wide MOF catalogue was done due to (see Table S1 and Figure S2): i) non-toxicity and availability of copper as metal centre and well-known trimesic acid chemistry as bridging organic ligand [36]; ii) suitable pore size [37] (9 Å) allowing the entrance and interaction of target FQs; iii) wide range of potential interaction forces

between sorbent and analytes such as hydrogen bonding (with amino, ketone or carboxylic groups), hydrophobic effects and π-interaction (between aromatic rings) and electrostatic interactions depending on pH (between surface composite charge and ionized groups from FQs). Bearing in mind all these considerations, the HKUST-1@polymer was evaluated as sorbent for microextraction in SPE-CE.

3.2. Characterization of the HKUST-1@polymer composite

An extensive characterization of the resulting composite was done in order to validate the synthesis and study its morphological, structural and chemical features.

Several techniques were applied for monitoring the correct formation of HKUST-1 onto the monolithic surface. As can be seen in the XRD patterns shown in Figure 1A, the typical peaks from the HKUST-1 simulated pattern appear at the final hybrid composite (from 10 to 30 º). Furthermore, at around 10º an intense signal corresponding to organic monolith can be observed, which suggests a higher proportion of polymer compared to HKUST-1. Figure 1B shows the FT-IR spectra over the range of 500–4000 cm^{-1}. As it can be observed, the characteristic peaks of HKUST-1 are present in the final composite (1600, 1550, 1375 and 750 cm^{-1}), but with lower intensities due to the smaller amount of MOF on the surface compared to polymeric network. Absorption of alkyl C-H stretch at 2900 cm^{-1} and carbonyl C=O stretch at 1750 cm^{-1} are originated from the methacrylate based polymer (for comparison of the composite and the bare monolith spectra, see Figure 1B). At the same time aromatic C=C bending is recognizable as a small band at 1600 cm^{-1}. In HKUST-1, C=O symmetric and asymmetric modes are present centered at 1625 cm^{-1} jointly with C=C aromatic bending. Both modes are clearly shown in the composite spectrum. FT-IR spectra from MOF precursors were also measured (Figure S3) in order to verify the HKUST-1 formation. Comparing the organic ligand and HKUST-1 spectra,

vibrational mode of -OH from carboxylic acids at 2500-3000 cm^{-1} disappears, which indicates the coordination between carboxylic acid and copper (II). Furthermore, in HKUST-1, bands of (C-O) and (C=O) are shifted to *ca.* 1375 and 1600 cm^{-1}, while in trimesic acid spectrum are originally placed at 1250 and 1700 cm^{-1}, respectively. This fact further confirmed the Cu(II) coordination.

Morphological exploration was carried out by electron microscopy. In the HRTEM micrograph of Figure 1C can be seen the homogeneous distribution of the HKUST-1 particles on the monolith surface. The particle size was ranging from 7 to 9 nm (n=25), which confirmed the nanosize of MOF crystals. The SEM image of Figure 1D reveals significant morphological differences compared to the typical globular shape of an organic monolith [12,38]. Clusters with spherical particles are depicted, with a rough surface due to the aggregation of HKUST-1 nano-domains (*ca.* size 45-55 nm). Information from both electronic microscopies agrees with the hypothesis of homogenous decoration on the surface due to the layer-by-layer strategy. The imaging analysis was continued with STEM-HAADF micrographs (Figure S4A) at $1.2 \cdot 10^6$X of magnification. In the sub-nano field, an average particle size of 4 nm (n=25) is observed for the HKUST-1 crystals in the HKUST-1@polymer. Furthermore, well-dispersed copper and, consequently MOF, is detected by EDX elemental mapping analysis as illustrated in a small area in Figure S4B. The EDX spectra also indicates a *ca.* 9% (m/m) of copper attached to the surface of the polymer. This detailed characterization was completed with the information from the N_2 adsorption isotherms obtained in a previous study [12]. N_2 isotherms clearly showed two adsorption steps from microporous (at low relative pressure) and macroporous (high relative pressure) behaviors due to MOF and monolithic natures, respectively. The surface area estimated with the BJH model for HKUST-1@polymer was 170 m^2g^{-1} vs 9 m^2g^{-1} for the bare monolith. All these facts support the

idea of a large active surface area of the hybrid composite, with a homogeneous distribution of the nano-MOF crystals throughout the polymer surface, ready to be accessible by the target analytes when applied as sorbent for microextraction in SPE-CE.

3.3. Development of the HKUST-1@polymer-SPE-CE-UV method

In order to achieve the highest analyte recoveries and detection sensitivity, several parameters affecting the method performance needed to be optimized using FQ standard mixtures. Since HKUST-1 was supposed to present limited stability if subjected to acidic pH for a long time, a neutral BGE was selected for the separation to ensure an extended lifetime. After some preliminary experiments by CE to check that an appropriate separation could be obtained for DAN, EFX and DFX with a 50 mM phosphate buffer at pH 7, the starting SPE-CE experiments were performed loading a 20 μg L^{-1} standard mixture in water for 5 min at 930 mbar followed by washing with BGE for 60 s at 930 mbar. One of the most important steps in a SPE procedure is the elution, which should be quantitative using the smallest volume of solvent to ensure high enrichment factors. The composition of the eluent was optimized injecting a volume of 10 s at 100 mbar. In all experiments, the plug of eluent was pushed from the inlet with BGE at 100 mbar for 60 s to improve repeatability between analyses and to avoid current disruption or failure. First, the MeOH content in the eluent was kept constant (90%, v/v) and H_2O:FA proportion was varied from 1 to 5% (v/v) of FA. The largest peak areas were obtained with 2% (v/v) of FA. A lower acid content led to a peak area diminution, and no FQs were detected without adding acid. In contrast higher acid contents did not produce a peak area increase but significant peak distortions. Using a 2% (v/v) of FA, the percentage of organic solvent in the eluent was studied for 80, 90 and 98% v/v of MeOH. As can be observed in Figure 2A, the largest peak areas were observed with a 98% (v/v) of MeOH.

Different experiments were performed to improve these results using MeCN and/or HAc. However, low repeatability, peak distortion and current breakdowns were observed. Therefore, a 2% (v/v) of FA in MeOH was selected as the optimized eluent. Regarding the elution solvent volume, a study varying the injection time from 5 to 15 s at 100 mbar was performed. Volumes injected greater than 10s (*ca.* 110 nL) caused current failure and were rapidly discarded. No differences on peak areas for the eluted FQs were found in the range between 5 and 10 s, and 5 s of eluent injection (*ca.* 50 nL) was selected to minimize the possibility of current breakdowns. To conclude the elution optimization, we investigated the pushing step of the elution plug from 15 to 90 s at 100 mbar. Non-significant differences were found in the peak areas while current was stable in all cases, hence 60 s was selected to ensure that the eluent plug already passed through the microcartridge before applying the separation voltage.

Under these elution conditions, the composition of sample loading was investigated introducing 20 µg L^{-1} standard mixtures in BGE (50 mM phosphate buffer at pH 7) or water (Figure S5). Peak areas were much larger with BGE, which was selected as loading composition. The influence of sample volume was investigated loading a 1 µg L^{-1} standard mixture at 930 mbar from 5 to 30 min (Figure S6A). The results showed that sorbent saturation and analyte breakthrough was not observed under the tested conditions, which suggested the suitability of the HKUST-1@polymer as a high extraction efficiency and large sample capacity sorbent for microscale applications. Saturation was neither observed when the standard mixture was loaded at 2 bar (see Figure S6B), but a significant reduction of microcartridge lifetime happened probably due to excessive sorbent packing. For further experiments, unless otherwise stated, 10 min at 930 mbar was set as sample loading conditions, as a good compromise between total analysis time, sensitivity enhancement and microcartridge durability.

Finally, the concentration of the BGE was also investigated at 25 mM and 75 mM phosphate (see Figure 2B). The 75 mM concentration was rapidly discarded because current values were excessive, the Ohm's law was not fulfilled and current failure was frequent. The best results in terms of peak area, repeatability and separation were achieved with the 50 mM concentration, since at 25 mM concentration DAN was not separated from the eluent components, which were migrating with the electroosmotic flow (EOF). Using the 50 mM phosphate (pH 7) BGE, several volumes were tested for washing after the loading step. At 930 mbar, duration times ranging from 30 to 90 s (*ca.* 3-9 µL) were tested (data not shown) and 60 s were enough to eliminate non-retained molecules and to fill the capillary before applying the separation voltage. Figures 3B and 3C show the SPE-CE electropherograms for 0.1 and 1 µg L^{-1} standard mixtures under the optimized conditions, respectively. As can be observed, an excellent sensitivity enhancement was obtained compared to the analysis of a 1000 µg L^{-1} standard mixture by CE (Figure 3C), without significant differences on peak efficiency or separation resolution. The excellent method performance would be mainly due to the specific structural and physicochemical features of the sorbent, but certain stacking effect during the elution could not be discarded to explain the high preconcentration factors [24].

In order to investigate the retention mechanism of the FQs in the HKUST-1@polymer under the optimized conditions, complementary Z-potential measurements were performed. As it can be seen in Figure S7, under the loading conditions at pH 7, the composite surface charge was negative (negative Z-potential value), while it was positive under the acidic elution conditions (positive Z-potential value). This suggested that at pH 7, when the zwitterionic FQs presented zero net charge (see pK_a values in Table S1), electrostatic interactions between the negatively charged composite and the cationic moieties of FQs would be governing retention. Besides, π-interactions between the

benzene rings within the composite and FQs would be also important. In contrast, at acidic pH when composite and FQs were positively charged, electrostatic repulsion favored FQ elution.

In order to evaluate non-specific retention, 20 μg L^{-1} standard mixtures were also analyzed by SPE-CE with microcartridges packed with the bare polymeric particles. Enhancements in the sensitivity of 80, 75 and 55% in terms of peak area were observed for DAN, EFX and DFX, respectively, with the HKUST-1@polymer compared to the bare monolith. Thus, these results demonstrated the key role of the nano-MOF in the efficient and selective extraction of FQs.

The optimized SPE-CE method was validated estimating the most relevant figures of merit. The method was linear between 0.1 and 80 μg L^{-1} (R^2> 0.992 for the three FQs), and LOD and LOQ were 0.03 and 0.1 μg L^{-1}, respectively. The LOD could be further decreased until 1 ng L^{-1} loading the sample for 30 min at 930 mbar (*ca.* 180 μL, or this volume at 2 bar for a shorter loading time) instead of for 10 min at 930 mbar (*ca.* 60 μL). These LOD values were 16,700 and 500,000 times lower than by CE-UV (0.5 mg L^{-1}), and they were low enough to detect FQs at trace levels. Intra-day repeatability with a single microcartridge was good: 4.0, 4.8 and 6.3% (% RSD of peak areas) for DAN, EFX and DFX, respectively. As expected, inter-day reproducibility with different microcartridges was slightly lower but acceptable: 6.7, 11.7 and 14.8% (% RSD of peak areas) for DAN, EFX and DFX, respectively. Finally, a microcartridge could be reused for 10 injections at 1 μg L^{-1} without a significant decrease on the extraction recoveries (R>80%), separation and current performance.

3.4. Application to real samples

For the analysis of FQs in real samples, several complex matrices were tested to confirm the wide applicability of the developed method. In order to avoid the microcartridge saturation, simple and fast sample pretreatments were necessary. Only adjustment to 50 mM phosphate pH 7, centrifugation and filtration were applied to river water, and an additional 1:10 dilution to human urine. Whole cow milk samples were deproteinized by acetonitrile precipitation, and the dried supernatants were treated in a similar way. Figures 4 A-C i) show the SPE-CE electropherograms for the blank samples. Since the FQs could not be detected in the blank samples, the samples were spiked at 1 μg L^{-1} with the standard mixture. Figures 4 A-C ii) illustrate the SPE-CE electropherograms of the spiked samples. As can be observed, the three FQs could be clearly detected after preconcentration without the interference of the rest of components from the sample matrix. Recoveries for the three FQs in the different samples under the optimized SPE-CE conditions are depicted in Table 1, and they ranged from 92 to 119% ($s<20\%$, $n=3$). These values suggested the validity of the proposed method to monitor drugs at trace levels in several complex matrices.

3.5. Comparison with other on-line automated methods

Finally, the developed HKUST-1@polymer-SPE-CE-UV method was compared with other relevant on-line automated approaches described in the literature [39–48] (see Table 2). At first glance, the use of sophisticated and expensive MS and MS/MS detection is a common practice in the analysis of FQs at trace level. However, the LOD by the developed method, which uses conventional and accessible UV detection, was much better or comparable to those achieved with expensive MS equipment [41,45–48]. Indeed, the obtained LOD was similar to the values reported with fluorescence detection [40,44],

which is widely recognized for the trace detection of FQs. This sensitivity, jointly with the facts that the fritless SPE-CE microcartridges are easily assembled with a few micrograms of sorbent and the system does not require valves for operation (see Table 2), underlines the convenience of using the developed method. Pang and co-workers developed an on-line SPE-HPLC method with fluorescence detection using as sorbent a layer-by-layer MOF@polymer [44]. In this case, several valves, pumps and fluorescence detection were required. Furthermore, 15 synthesis cycles were necessary to prepare the MOF to obtain comparable LOD values to our study, which required only 4 cycles. Regarding the method precision, the RSD values were similar in all cases except for those obtained with certain approaches, which were slightly higher [45,46]. Another convenient feature of the developed method was the small sample volume required. Excepting for those methods based on SPE-CE [46–48], sample volumes larger than 1 mL were needed, which would suppose a drawback with samples of limited availability (e.g. biological fluids). To conclude the comparison, the recovery values were in general ranging between 70 and 125% excepting for a few studies affected by matrix effects [41,46]. Globally, the developed HKUST-1@monolith-SPE-CE-UV method can be regarded as an attractive and highly recommendable alternative for determination of FQs in complex samples.

4. Conclusions

An HKUST-1 nano-MOF was built layer-by-layer onto the surface of an organic polymer resulting in a hybrid composite that was carefully characterized and used for the first time as sorbent for SPE-CE-UV. The suitability of the HKUST-1@polymer as a highly efficient and versatile sorbent for microextraction has been demonstrated by analyzing FQs at trace levels in river water, human urine and whole cow milk samples. The large active surface area and morphology of the hybrid composite allowed the rapid and simple

preparation of fritless particle-packed microcartridges and sensitivity enhancements up to 500,000 times compared to CE-UV, with minute sample loading (≤ 180 µL). The performance of the method regarding linearity, repeatability, reproducibility, durability and recoveries or matrix effect with real samples was also remarkable. Furthermore, it could be easily adapted to analyze other ionizable and non-ionizable drugs or biomarkers considering the mechanisms governing retention and elution from the hybrid composite. Beyond SPE-CE, the achieved unprecedented sensitivity enhancement and appropriate selectivity could expand the applicability of nano-MOF@polymer composites in other microextraction techniques.

Acknowledgments

This study was supported by the Ministry of Ministry of Science, Innovation and Universities of Spain (MSIU) of Spain (RTI2018-095536-B-I00 and RTI2018-097411-B-I00) and the Cathedra UB Rector Francisco Buscarons Úbeda (Forensic Chemistry and Chemical Engineering). F. Benavente acknowledges the Vice-rectorate for Research of the University of Valencia for a visiting researcher fellowship (*Atracción de Talento* program). H. Martínez-Pérez-Cejuela thanks the MSIU for a PhD FPU grant. The authors extend their appreciation to MSIU for granting the Spanish Network of Excellence in Sample preparation (RED2018-102522-T). This research is performed in the framework of the Sample Preparation Task Force and Network, supported by the Division of Analytical Chemistry of the European Chemical Society.

Author contributions:

All authors contributed to conceptualization of this manuscript.

-Héctor Martínez-Pérez-Cejuela: methodology and design, formal analysis and investigation, writing-original draft and revision

-Fernando Benavente: methodology and design, writing-review and editing, supervision, funding acquisition

-Ernesto F. Simó-Alfonso: writing-review and editing, supervision, funding acquisition and resources

-José M. Herrero-Martínez: writing-review and editing, supervision, funding acquisition and resources

Notes

The authors declare no competing financial interest.

References

[1] H. Furukawa, K.E. Cordova, M. O'Keeffe, O.M. Yaghi, The chemistry and applications of metal-organic frameworks, Science (80-.). 341 (2013) 1230444. https://doi.org/10.1126/science.1230444.

[2] M. Safaei, M.M. Foroughi, N. Ebrahimpoor, S. Jahani, A. Omidi, M. Khatami, A review on metal-organic frameworks: Synthesis and applications, TrAC - Trends Anal. Chem. 118 (2019) 401–425. https://doi.org/10.1016/j.trac.2019.06.007.

[3] Z.Y. Gu, C.X. Yang, N. Chang, X.P. Yan, Metal-organic frameworks for analytical chemistry: From sample collection to chromatographic separation, Acc. Chem. Res. 45 (2012) 734–745. https://doi.org/10.1021/ar2002599.

[4] F.A. Hansen, S. Pedersen-Bjergaard, Emerging Extraction Strategies in Analytical Chemistry, Anal. Chem. 92 (2020) 2–15. https://doi.org/10.1021/acs.analchem.9b04677.

[5] M.Y. Masoomi, A. Morsali, P.C. Junk, Ultrasound assisted synthesis of a Zn(ii) metal-organic framework with nano-plate morphology using non-linear dicarboxylate and linear N-donor ligands, RSC Adv. 4 (2014) 47894–47898. https://doi.org/10.1039/c4ra09186h.

[6] Y.V. Kaneti, J. Tang, R.R. Salunkhe, X. Jiang, A. Yu, K.C.W. Wu, Y. Yamauchi, Nanoarchitectured Design of Porous Materials and Nanocomposites from Metal-Organic Frameworks, Adv. Mater. 29 (2017) 1604898. https://doi.org/10.1002/adma.201604898.

[7] F. Bigdeli, F. Rouhani, A. Morsali, A. Ramazani, Ultrasonic-assisted synthesis of the nanostructures of a Co(II) metal organic framework as a highly sensitive fluorescence probe of phenol derivatives, Ultrason. Sonochem. 62 (2020) 104862. https://doi.org/10.1016/j.ultsonch.2019.104862.

[8] A. Khoobi, M. Salavati-Niasari, M. Ghani, S.M. Ghoreishi, A. Gholami, Multivariate optimization methods for in-situ growth of LDH/ZIF-8 nanocrystals on anodized aluminium substrate as a nanosorbent for stir bar sorptive extraction in biological and food samples, Food Chem. 288 (2019) 39–46. https://doi.org/10.1016/j.foodchem.2019.02.118.

[9] T. Wiwasuku, J. Othong, J. Boonmak, V. Ervithayasuporn, S. Youngme, Sonochemical synthesis of microscale Zn(ii)-MOF with dual Lewis basic sites for fluorescent turn-on detection of Al3+and methanol with low detection limits, Dalt. Trans. 49 (2020) 10240–10249. https://doi.org/10.1039/d0dt01175d.

[10] H. Martínez-Pérez-Cejuela, Ó. Mompó-Roselló, N. Crespí-Sánchez, C. Palomino Cabello, M. Catalá-Icardo, E.F. Simó-Alfonso, J.M. Herrero-Martínez, Determination of benzomercaptans in environmental complex samples by combining zeolitic imidazolate framework-8-based solid-phase extraction and high-performance liquid chromatography with UV detection, J. Chromatogr. A. 1631 (2020) 461580. https://doi.org/10.1016/j.chroma.2020.461580.

[11] S. Wang, Y. Lv, Y. Yao, H. Yu, G. Lu, Modulated synthesis of monodisperse MOF-5 crystals with tunable sizes and shapes, Inorg. Chem. Commun. 93 (2018) 56–60. https://doi.org/10.1016/j.inoche.2018.05.010.

[12] H. Martínez-Pérez-Cejuela, M. Guiñez, E.F. Simó-Alfonso, P. Amorós, J. El Haskouri, J.M. Herrero-Martínez, In situ growth of metal-organic framework HKUST-1 in an organic polymer as sorbent for nitrated and oxygenated polycyclic aromatic hydrocarbon in environmental water samples prior to quantitation by HPLC-UV, Microchim. Acta. 187 (2020) 301. https://doi.org/10.1007/s00604-020-04265-z.

[13] M. Shokrollahi, S. Seidi, L. Fotouhi, In situ electrosynthesis of a copper-based

metal–organic framework as nanosorbent for headspace solid-phase microextraction of methamphetamine in urine with GC-FID analysis, Microchim. Acta. 187 (2020) 548. https://doi.org/10.1007/s00604-020-04535-w.

[14] R. Li, S. Li, Q. Zhang, Y. Li, H. Wang, Layer-by-layer assembled triphenylene-based MOFs films for electrochromic electrode, Inorg. Chem. Commun. (2020) 108354. https://doi.org/10.1016/j.inoche.2020.108354.

[15] J. Zhao, B. Gong, W.T. Nunn, P.C. Lemaire, E.C. Stevens, F.I. Sidi, P.S. Williams, C.J. Oldham, H.J. Walls, S.D. Shepherd, M.A. Browe, G.W. Peterson, M.D. Losego, G.N. Parsons, Conformal and highly adsorptive metal-organic framework thin films via layer-by-layer growth on ALD-coated fiber mats, J. Mater. Chem. A. 3 (2015) 1458–1464. https://doi.org/10.1039/c4ta05501b.

[16] Y. Lv, X. Tan, F. Svec, Preparation and applications of monolithic structures containing metal–organic frameworks, J. Sep. Sci. 40 (2017) 272–287. https://doi.org/10.1002/jssc.201600423.

[17] N. Stock, S. Biswas, Synthesis of metal-organic frameworks (MOFs): Routes to various MOF topologies, morphologies, and composites, Chem. Rev. 112 (2012) 933–969. https://doi.org/10.1021/cr200304e.

[18] Wahiduzzaman, K. Allmond, J. Stone, S. Harp, K. Mujibur, Synthesis and Electrospraying of Nanoscale MOF (Metal Organic Framework) for High-Performance CO2 Adsorption Membrane, Nanoscale Res. Lett. 12 (2017) 1–12. https://doi.org/10.1186/s11671-016-1798-6.

[19] X. Zhong, Y. Zhang, L. Tan, T. Zheng, Y. Hou, X. Hong, G. Du, X. Chen, Y. Zhang, X. Sun, An aluminum adjuvant-integrated nano-MOF as antigen delivery system to induce strong humoral and cellular immune responses, J. Control. Release. 300 (2019) 81–92. https://doi.org/10.1016/j.jconrel.2019.02.035.

[20] S. Homayoonnia, S. Zeinali, Design and fabrication of capacitive nanosensor based on MOF nanoparticles as sensing layer for VOCs detection, Sensors Actuators, B Chem. 237 (2016) 776–786. https://doi.org/10.1016/j.snb.2016.06.152.

[21] A. Herbst, A. Khutia, C. Janiak, Brønsted instead of lewis acidity in functionalized MIL-101Cr MOFs for efficient heterogeneous (nano-MOF) catalysis in the condensation reaction of aldehydes with alcohols, Inorg. Chem. 53 (2014) 7319–7333. https://doi.org/10.1021/ic5006456.

[22] S.A. Kitte, T.H. Fereja, M.I. Halawa, B. Lou, H. Li, G. Xu, Recent advances in nanomaterial-based capillary electrophoresis, Electrophoresis. 40 (2019) 2050–2057. https://doi.org/10.1002/elps.201800534.

[23] R.L.C. Voeten, I.K. Ventouri, R. Haselberg, G.W. Somsen, Capillary Electrophoresis: Trends and Recent Advances, Anal. Chem. 90 (2018) 1464–1481. https://doi.org/10.1021/acs.analchem.8b00015.

[24] M.C. Breadmore, W. Grochocki, U. Kalsoom, M.N. Alves, S.C. Phung, M.T. Rokh, J.M. Cabot, A. Ghiasvand, F. Li, A.I. Shallan, A.S.A. Keyon, A.A. Alhusban, H.H. See, A. Wuethrich, M. Dawod, J.P. Quirino, Recent advances in enhancing the sensitivity of electrophoresis and electrochromatography in capillaries and microchips (2016–2018), Electrophoresis. 40 (2019) 17–39. https://doi.org/10.1002/elps.201800384.

[25] L. Pont, R. Pero-Gascon, E. Gimenez, V. Sanz-Nebot, F. Benavente, A critical retrospective and prospective review of designs and materials in in-line solid-phase extraction capillary electrophoresis, Anal. Chim. Acta. 1079 (2019) 1–19. https://doi.org/10.1016/j.aca.2019.05.022.

[26] L. Pont, F. Benavente, J. Barbosa, V. Sanz-Nebot, On-line immunoaffinity solid-phase extraction capillary electrophoresis mass spectrometry using Fab´antibody

fragments for the analysis of serum transthyretin, Talanta. 170 (2017) 224–232. https://doi.org/10.1016/j.talanta.2017.03.104.

[27] R. Pero-Gascon, V. Sanz-Nebot, M. V. Berezovski, F. Benavente, Analysis of Circulating microRNAs and Their Post-Transcriptional Modifications in Cancer Serum by On-Line Solid-Phase Extraction-Capillary Electrophoresis-Mass Spectrometry, Anal. Chem. 90 (2018) 6618–6625. https://doi.org/10.1021/acs.analchem.8b00405.

[28] R. Pero-Gascon, F. Benavente, Z. Minic, M. V. Berezovski, V. Sanz-Nebot, On-line Aptamer Affinity Solid-Phase Extraction Capillary Electrophoresis-Mass Spectrometry for the Analysis of Blood α-Synuclein, Anal. Chem. 92 (2020) 1525–1533. https://doi.org/10.1021/acs.analchem.9b04802.

[29] L. Pont, G. Marin, M. Vergara-Barberán, L.G. Gagliardi, V. Sanz-Nebot, J.M. Herrero-Martínez, F. Benavente, Polymeric monolithic microcartridges with gold nanoparticles for the analysis of protein biomarkers by on-line solid-phase extraction capillary electrophoresis-mass spectrometry, J. Chromatogr. A. 1622 (2020) 461097. https://doi.org/10.1016/j.chroma.2020.461097.

[30] H.H. Lauer, Rozing G.P., High performance capillary electrophoresis, 2nd Ed., Pags. 60-61, Waldbronn, Germany, 2014.

[31] T. Hong, W. Liu, M. Li, C. Chen, Click chemistry at the microscale, Analyst. 144 (2019) 1492–1512. https://doi.org/10.1039/c8an01497c.

[32] Y. Xu, Q. Cao, F. Svec, J.M.J. Fréchet, Porous polymer monolithic column with surface-bound gold nanoparticles for the capture and separation of cysteine-containing peptides, Anal. Chem. 82 (2010) 3352–3358. https://doi.org/10.1021/ac1002646.

[33] F. Maya, C. Palomino Cabello, J.M. Estela, V. Cerdà, G. Turnes Palomino,

Automatic In-Syringe Dispersive Microsolid Phase Extraction Using Magnetic Metal-Organic Frameworks, Anal. Chem. 87 (2015) 7545–7549. https://doi.org/10.1021/acs.analchem.5b01993.

[34] S. Yang, F. Ye, Q. Lv, C. Zhang, S. Shen, S. Zhao, Incorporation of metal-organic framework HKUST-1 into porous polymer monolithic capillary columns to enhance the chromatographic separation of small molecules, J. Chromatogr. A. 1360 (2014) 143–149. https://doi.org/10.1016/j.chroma.2014.07.067.

[35] M. Giesbers, E.J. Carrasco-Correa, E.F. Simó-Alfonso, J.M. Herrero-Martínez, Hybrid monoliths with metal-organic frameworks in spin columns for extraction of non-steroidal drugs prior to their quantitation by reversed-phase HPLC, Microchim. Acta. 186 (2019) 759 (1–9). https://doi.org/10.1007/s00604-019-3923-6.

[36] M.H. Yap, K.L. Fow, G.Z. Chen, Synthesis and applications of MOF-derived porous nanostructures, Green Energy Environ. 2 (2017) 218–245. https://doi.org/10.1016/j.gee.2017.05.003.

[37] Y. Mao, G. Li, Y. Guo, Z. Li, C. Liang, X. Peng, Z. Lin, Foldable interpenetrated metal-organic frameworks/carbon nanotubes thin film for lithium-sulfur batteries, Nat. Commun. 8 (2017) 14628. https://doi.org/10.1038/ncomms14628.

[38] H.M. Pérez-Cejuela, E.J. Carrasco-Correa, A. Shahat, E.F. Simó-Alfonso, J.M. Herrero-Martínez, Incorporation of metal-organic framework amino-modified MIL-101 into glycidyl methacrylate monoliths for nano LC separation, J. Sep. Sci. 42 (2019) 834–842. https://doi.org/10.1002/jssc.201801135.

[39] A. Prieto, S. Schrader, C. Bauer, M. Möder, Synthesis of a molecularly imprinted polymer and its application for microextraction by packed sorbent for the determination of fluoroquinolone related compounds in water, Anal. Chim. Acta.

685 (2011) 146–152. https://doi.org/10.1016/j.aca.2010.11.038.

[40] E. Rodríguez, F. Navarro-Villoslada, E. Benito-Peña, M.D. Marazuela, M.C. Moreno-Bondi, Multiresidue determination of ultratrace levels of fluoroquinolone antimicrobials in drinking and aquaculture water samples by automated online molecularly imprinted solid phase extraction and liquid chromatography, Anal. Chem. 83 (2011) 2046–2055. https://doi.org/10.1021/ac102839n.

[41] L. Kantiani, M. Farré, D. Barceló, Rapid residue analysis of fluoroquinolones in raw bovine milk by online solid phase extraction followed by liquid chromatography coupled to tandem mass spectrometry, J. Chromatogr. A. 1218 (2011) 9019–9027. https://doi.org/10.1016/j.chroma.2011.09.079.

[42] A. Manbohi, S.H. Ahmadi, In-tube magnetic solid phase microextraction of some fluoroquinolones based on the use of sodium dodecyl sulfate coated Fe3O4 nanoparticles packed tube, Anal. Chim. Acta. 885 (2015) 114–121. https://doi.org/10.1016/j.aca.2015.05.030.

[43] C. Vakh, M. Alaboud, S. Lebedinets, D. Korolev, V. Postnov, L. Moskvin, O. Osmolovskaya, A. Bulatov, An automated magnetic dispersive micro-solid phase extraction in a fluidized reactor for the determination of fluoroquinolones in baby food samples, Anal. Chim. Acta. 1001 (2018) 59–69. https://doi.org/10.1016/j.aca.2017.11.065.

[44] J. Pang, Y. Liao, X. Huang, Z. Ye, D. Yuan, Metal-organic framework-monolith composite-based in-tube solid phase microextraction on-line coupled to high-performance liquid chromatography-fluorescence detection for the highly sensitive monitoring of fluoroquinolones in water and food samples, Talanta. 199 (2019) 499–506. https://doi.org/10.1016/j.talanta.2019.03.019.

[45] M. Tang, Y. Zhao, J. Chen, D. Xu, On-line multi-residue analysis of

fluoroquinolones and amantadine based on integrated microfluidic chip coupled to triple quadrupole mass spectrometry, Anal. Methods. (2020). https://doi.org/10.1039/d0ay01641a.

[46] F.J. Lara, A.M. García-Campaña, F. Alés-Barrero, J.M. Bosque-Sendra, In-line solid-phase extraction preconcentration in capillary electrophoresis-tandem mass spectrometry for the multiresidue detection of quinolones in meat by pressurized liquid extraction, Electrophoresis. 29 (2008) 2117–2125. https://doi.org/10.1002/elps.200700666.

[47] G. Morales-Cid, S. Cárdenas, B.M. Simonet, M. Valcárcel, Fully automatic sample treatment by integration of microextraction by packed sorbents into commercial capillary electrophoresis-mass spectrometry equipment: Application to the determination of fluoroquinolones in urine, Anal. Chem. 81 (2009) 3188–3193. https://doi.org/10.1021/ac900234j.

[48] D. Moreno-González, F.J. Lara, L. Gámiz-Gracia, A.M. García-Campaña, Molecularly imprinted polymer as in-line concentrator in capillary electrophoresis coupled with mass spectrometry for the determination of quinolones in bovine milk samples, J. Chromatogr. A. 1360 (2014) 1–8. https://doi.org/10.1016/j.chroma.2014.07.049.

Figure captions

Figure 1. Characterization studies of HKUST-1@polymer. A) Powder XRD pattern profiles of the bare polymer, the hybrid composite and the simulated HKUST-1 MOF; B) FT-IR spectra (4000-500cm^{-1}) of the hybrid composite, the bare polymer and the HKUST-1 MOF; C) HRTEM and D) SEM micrographs of the hybrid composite.

Figure 2. SPE-CE-UV method optimization with a 20 µg L^{-1} standard mixture of FQs. A) Effect of the eluent composition on the peak areas of the FQs (MeOH:H_2O:FA, v/v/v) and B) electropherograms (280 nm) with different concentration of phosphate BGE at pH 7. Peak identification: 1) DAN, 2) EFX and 3) DFX. The rest of experimental conditions (optimized method) are given in the experimental section.

Figure 3. Electropherograms (280 nm) for standard mixtures of FQs at different concentrations by CE-UV (A) and SPE-CE-UV (B and C). Peak identification: 1) DAN; 2) EFX; 3) DFX. The rest of experimental conditions (optimized method) are given in the experimental section.

Figure 4. SPE-CE-UV electropherograms (280 nm) for A) river water, B) human urine and C) whole cow milk (i) blank samples and (ii) spiked samples with FQs at 1µg L^{-1}. Peak identification: 1) DAN; 2) EFX; 3) DFX. The experimental conditions (optimized method) are given in the experimental section.

Table 1. Recoveries of FQs at 1 μg L^{-1} spiked concentration in real samples by HKUST-1@polymer-SPE-CE-UV (n = 3, s=standard deviation).

Sample	Analyte	Recovery, % (±s)
River water	DAN	100 (± 4)
	EFX	92 (± 12)
	DFX	100 (± 14)
Urine	DAN	113.1 (± 0.9)
	EFX	102 (± 3)
	DFX	108 (± 2)
Milk	DAN	103 (± 10)
	EFX	106 (± 19)
	DFX	119 (± 8)

Table 2. Comparison of the developed SPE-CE-UV method with other relevant on-line automated methods reported in the literature.

Material (amount)[a]	Sample matrix	Method[b]	Sample volume (mL)	LOD (ng L^{-1})	Recovery (%)	Precision (RSD, %)	Ref.
MIP (4mg)	Water	SPE-LC-MS/MS (v)	1.6	0.5-3.8	93-115	<13	[39]
MIP (40mg)	Water	SPE-LC-FLD (v)	25	1-12	93-102	<6	[40]
PLRP (tens of mg)	Milk	SPE-LC-MS/MS (v)	0.3	30-4230	65-123	<7	[41]
Fe_3O_4 (10µg)	Water and urine	MSPE-HPLC-UV (v)	15	10-50	92-106	<5	[42]
Zr-Fe-C (5mg)	Baby food	MSPE-HPLC-FLD (v)	-	1500-3000	86-122	<10	[43]
ZIF-8@monolith (tens of mg)	Water and honey	SPE-HPLC-FLD (v)	16	0.14-1.1	80-119	<10	[44]
HLB (18mg)	Chicken	FSPE-chip-QQQ-MS	-	44-107	85-122	≤20	[45]
MCX (100µg)[a]	Chicken	SPE-CE-MS/MS	-	17-59	63-112	≤20	[46]
C18 (4mg)	Urine	SPE-CE-MS (v)	0.24	6300-10600	71-109	<6	[47]
MIP (100µg)[a]	Milk	SPE-CE-MS/MS	0.022	1000–1400ng kg^{-1}	70-102	≤11	[48]
HKUST-1@polymer (100µg)[a]	Water, urine, milk	SPE-CE-UV	0.06 (10min 930mbar) 0.18 (30 min 930 mbar)	30 1	92-119	<14	This study

Abbreviations: MIP, molecularly imprinted polymer; PLRP, polymeric reversed-phase sorbent; ZIF-8: zeolitic imidazolate framework-8; HLB, hydrophilic-lipophilic balance; MCX, mixed-mode polymeric sorbent; HKUST-1, Hong Kong university of science and technology-1; SPE: solid-phase extraction; LC-MS/MS, liquid chromatography coupled to tandem mass spectrometry; FLD: fluorescence detection; MSPE: magnetic SPE; FSPE-chip-QQQ-MS, fluidic solid-phase extraction with chip triple quadrupole mass spectrometry; UV, ultraviolet detection.

[a]The amount of material was estimated in SPE-CE without valves.

[b] (v)= the instrumental set-up requires valves

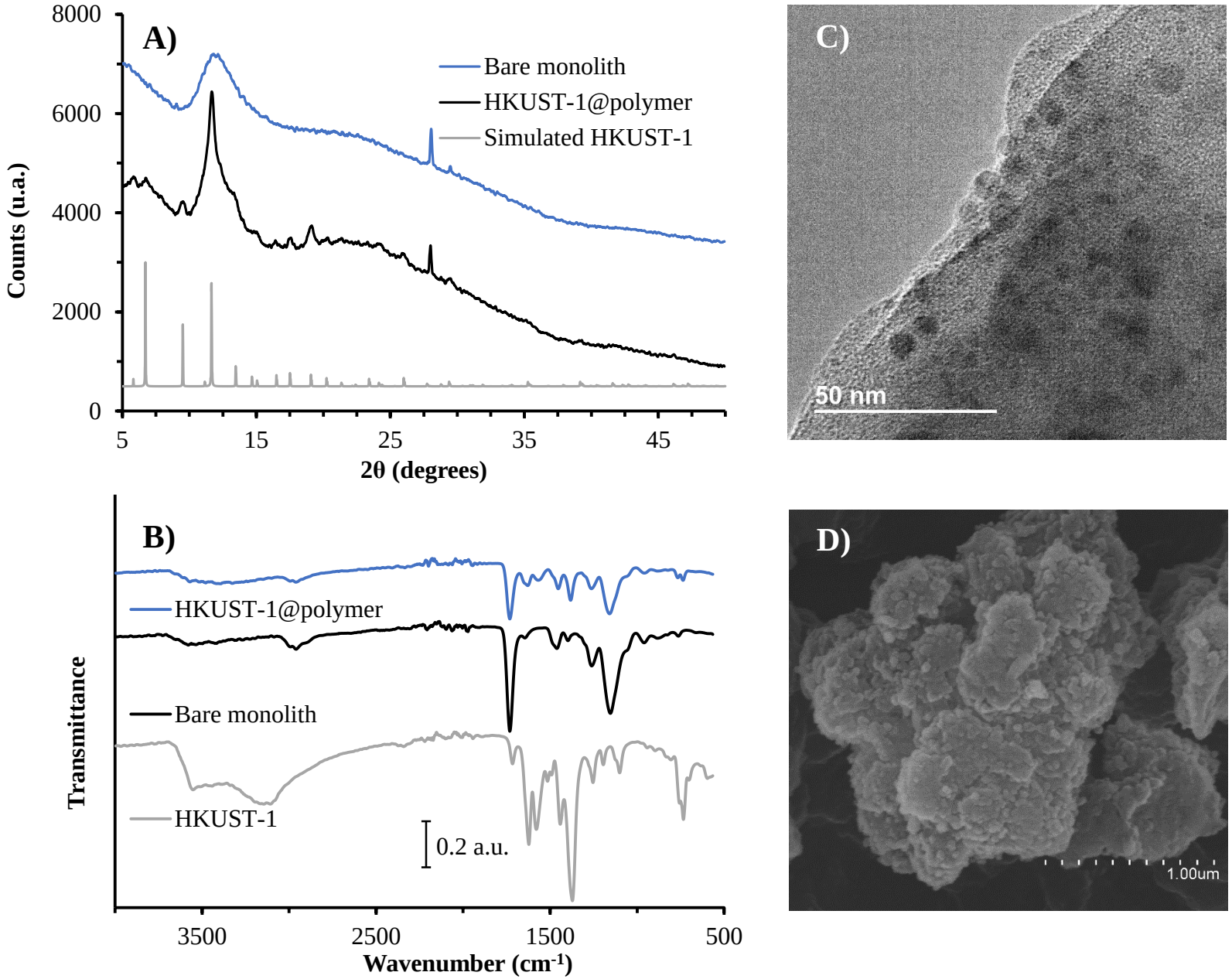

Figure 1. Martínez-Pérez-Cejuela et al.

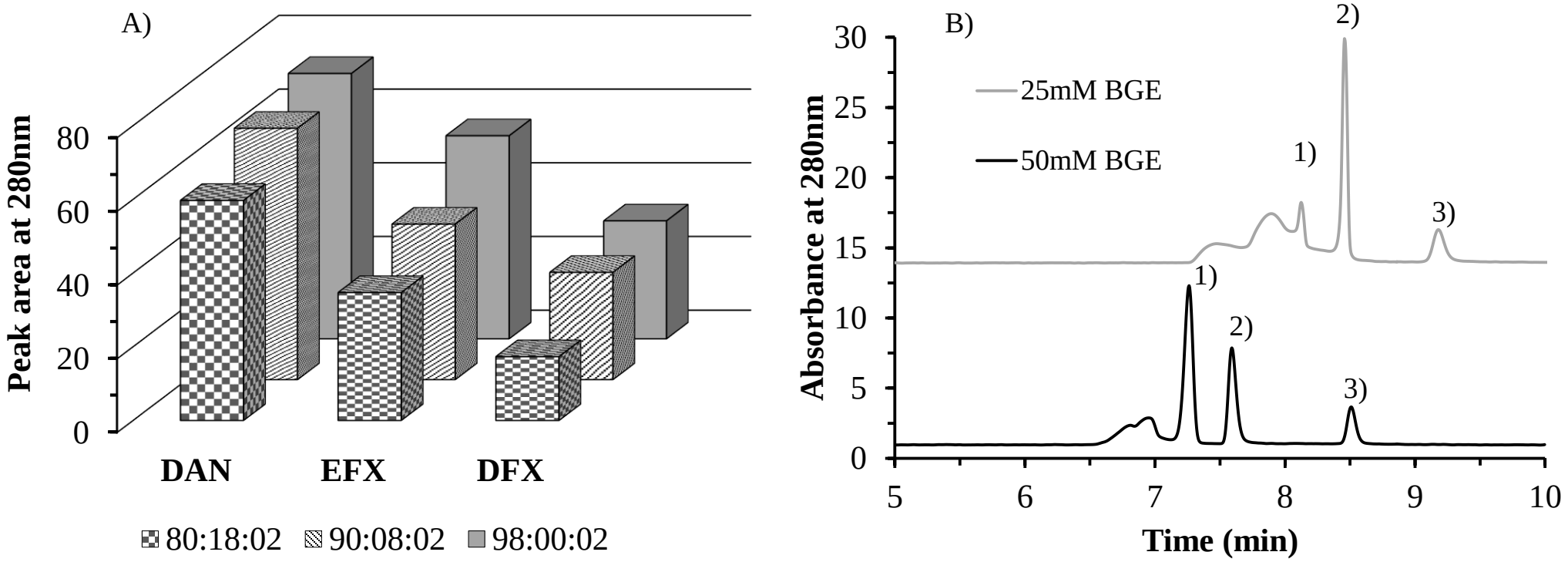

Figure 2. Martínez-Pérez-Cejuela et al.

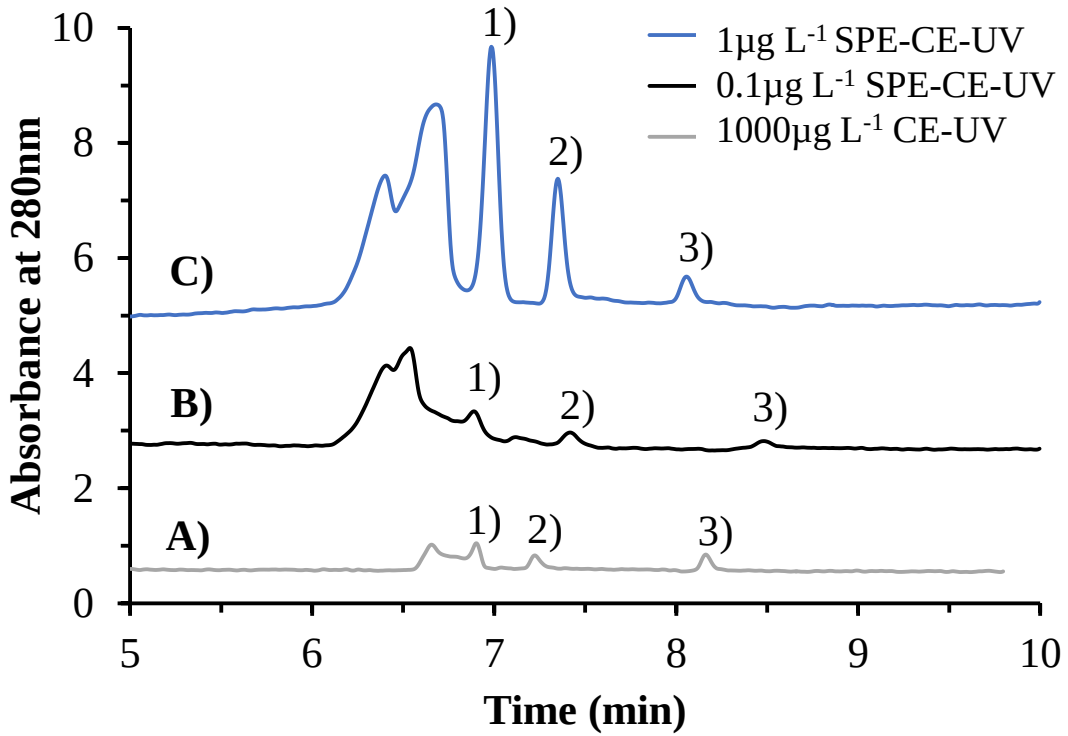

Figure 3. Martínez-Pérez-Cejuela et al.

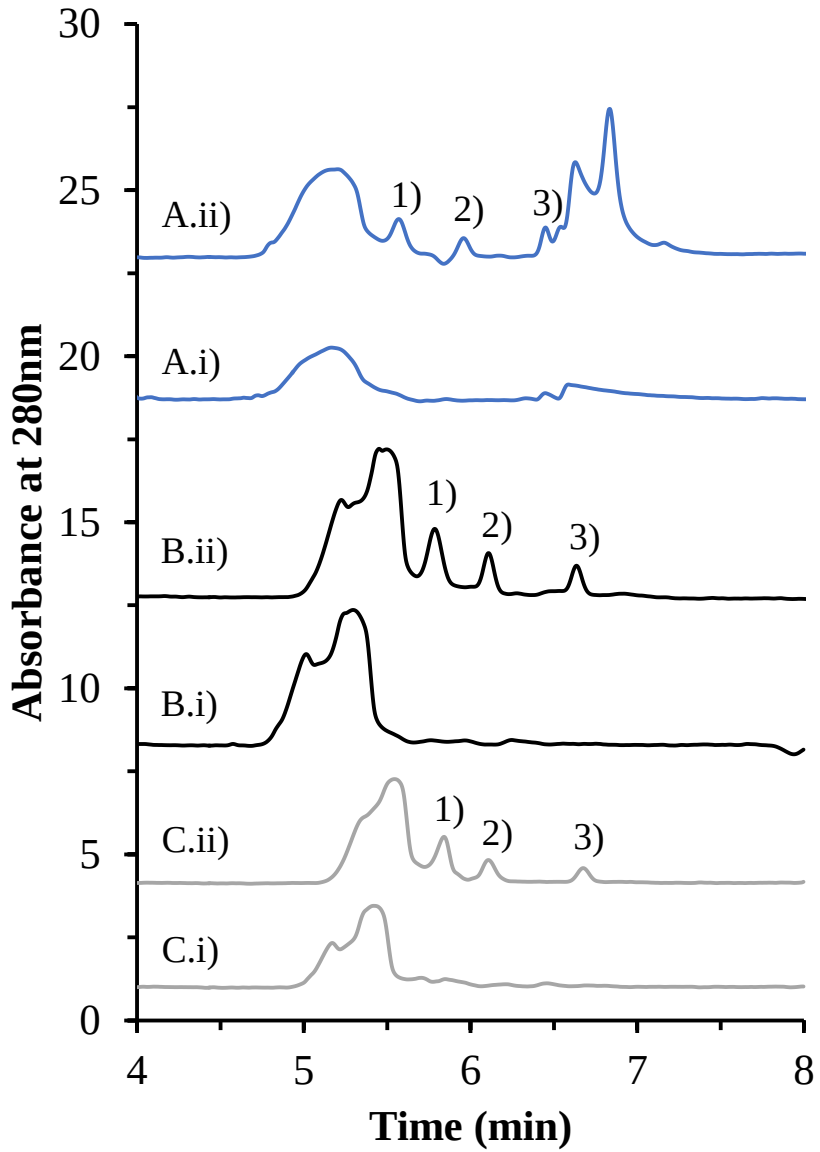

Figure 4. Martínez-Pérez-Cejuela et al.

ELECTRONIC SUPPLEMENTARY MATERIAL FOR

A hybrid nano-MOF/polymer material for trace analysis of fluoroquinolones in complex matrices at microscale by on-line solid-phase extraction capillary electrophoresis

Héctor Martínez-Pérez-Cejuela[1], Fernando Benavente[2]*, Ernesto F. Simó-Alfonso[1], José M. Herrero-Martínez[1]*

[1]*Department of Analytical Chemistry, University of Valencia, c/Dr. Moliner, 50, 46100-Burjassot, Valencia (Spain).*

[2]*Department of Chemical Engineering and Analytical Chemistry, Institute for Research on Nutrition and Food Safety (INSA·UB), University of Barcelona, Barcelona, Spain*

*Prof. José Manuel Herrero Martínez, e-mail: jmherrer@uv.es; Tel: +34963544062; Fax: +34963544436

*Prof. Fernando Benavente, e-mail fbenavente@ub.edu; Tel: +34934035423,; Fax: +34934021233

Table of contents

Reagents and materials

All the reagents and solvents were at least analytical grade.

Copper (II) acetate monohydrate ($Cu(AcO)_2 \cdot H_2O$), trimesic acid (H_3BTC), methacrylic acid (MAA), ethylene glycol dimethacrylate (EDMA), dimethyl sulfoxide (DMSO), 2, 2'-azobisisobutyronitrile (AIBN) were obtained from Sigma-Aldrich (St. Louis, MO, USA), while polyethylene glycol 6000 (PEG 6000) was supplied by Fluka (Buchs SG, Switzerland). FQs (see Table S1) were: danofloxacin (DAN) enrofloxacin (EFX) y difloxacin (DFX) and all of them were provided by Sigma-Aldrich. Hydrochloric acid, sodium hydroxide, HPLC-grade methanol (MeOH) and acetonitrile (MeCN) were supplied by VWR Chemicals (Barcelona, Spain). Ethanol (EtOH) was purchased from Scharlab (Barcelona, Spain). Formic acid (FA) and acetic acid were purchased from Sigma Aldrich, whereas sodium phosphate salts (Na_2HPO_4 and NaH_2PO_4) were from Fisher Scientific (Madrid, Spain).

Individual stock solutions (1,000 mg L^{-1}) of each FQ were prepared in MeOH using amber glass vials and stored at 4ºC for not more than a month. A methanolic stock solution mixture of 100 mg L^{-1} was prepared weekly and working solution mixtures were prepared daily diluting with separation background electrolyte (BGE).

Fusedsilica capillaries were purchased from Polymicro Technologies (Phoenix, AZ, USA). Bi-component epoxy-resin SuperTite® (Supertite Sam, S.L., Almussafes, Valencia) was purchased in a local hardware store. Nanopure water (Crystal B30 EDI Adrona deionizer, Riga, Latvia) was used with conductivity value and total organic carbon lower than 18.2 MΩ cm^{-1} and 2 μg L^{-1}, respectively.

River water was collected from Turia river (39°30'14.7"N 0°28'25.2"W, Valencia). A clean catch first-morning urine sample was obtained from a healthy donor (male, 25) according to the ethical guidelines of the University of Valencia. Whole cow milk was

purchased in a local supermarket. All the samples were kept in amber glass vials and refrigerated at 4ºC until their use.

Instruments and apparatus

Scanning electron microscopy (SEM) micrographs were recorded with a Hitachi microscope (S-4800, Ibaraki, Japan) with retro-dispersive electron detector. Before analysis, the materials were sputter coated with a thin layer of Au/Pd under a nitrogen stream at low pressure.

For high resolution transmission electron microscopy (HRTEM), a carbon coated nickel microgrid was used, where an ethanolic dispersion of the samples was deposited. Before observation, the samples were dried with an air stream. HRTEM imaging adquisition was carried out in a JEOL microscope (JEM 2100F, Freising, Germany) working at 200kV. A high resolution CCD camera GATAN SC-200, achieving a point resolution of 0.19nm, and an EDX detector (X-Max 80, Oxford Instruments, Wiesbaden, Germany) to perform point and area chemical analyses were coupled to the instrument.

A similar material pretreatment and the same microscope and detectors were used for scanning transmission electron microscopy (STEM) with high-angle annular dark-field imaging (STEM-HAADF).

Powder X-ray diffraction (XRD) patterns were registered in a D8 Advance A25 diffractometer (Bruker Daltonik GmbH, Bremen, Germany) with experimental conditions of 40 mA and 40 kV in each analysis. A single diffractogram acquired at room temperature from $2\theta = 5°$ to $2\theta = 50°$ is the average of five repeated measurements.

For attenuated total reflection Fourier-transform infrared (FT-IR) spectra, homogenous powdered materials were placed on the FT-IR Tensor 27 spectrometer (Bruker Daltonik).

A DuraSamplIR II accessory (Smiths Detection Inc., Warrington, UK) with a nine reflection diamond/ZnSe DuraDisk plate was coupled to the spectrometer.

In the zeta potential studies, a Zetasizer Nano ZS equipment (Malvern Instruments, Malvern, UK) was used. The hybrid material was dispersed in the optimized solvents for loading (BGE 50 mM phosphate pH 7) and elution (2% (v/v) FA in MeOH) in SPE-CE at a concentration of 100 mg L^{-1} and sonicated for 90 s. The analysis was performed in triplicate at room temperature. Zeta potential value was calculated from the particle mobility by applying the Smoluchowski model as recommended by the manufacturer.

CE and SPE-CE experiments were conducted in a 7100 CE system equipped with a diode array spectrophotometric detector (Agilent Technologies, Waldbronn, Germany). ChemStation software (Agilent Technologies) was used for instrument control and data acquisition.

The material synthesis was monitored using an 8453 diode-array UV-vis spectrophotometer (Agilent Technologies). pH values were measured with a Crison GLP 21 potentiometer (Crison Instruments, Barcelona, Spain) and a Metria electrode (Labbox Labware, S.L., Barcelona, Spain). The vacuum for sorbent packing was performed with a N938 mini laboratory pump Laboport (KNF, Freiburg, Germany). Microcartridge assembling was supervised using a DM 400 USB digital microscope (Bresser GmbH, Berlin, Germany). Evaporation under vacuum was conducted using a miVac sample concentrator (SP Scientific, PA, USA). Magnetic stirring was performed using a LBX S01 magnetic stirrier (Labbox Labware)

Table S1. Structures and physicochemical properties of fluoroquinolones (FQs).

Compound	Structure	Log $P_{O/W}$*	pK_{a1}*	pK_{a2}*	MRLs* (milk)
Danofloxacin (DAN)	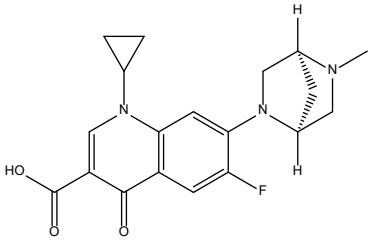	0.71	6.07	8.56	30 μg kg^{-1}
Enrofloxacin (EFX)	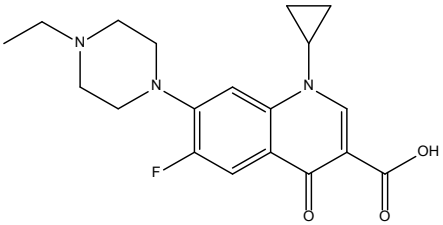	1.15	5.88	7.74	100 μg kg^{-1}**
Difloxacin (DFX)	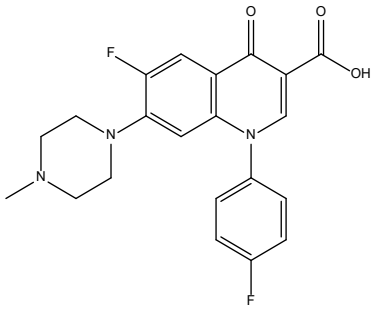	1.16	5.66	7.24	Not allowed***

*Values of Log $P_{O/W}$ were predicted with ChemAxon software (11/20/2020, ChemAxon, Budapest, Hungary); values of pKas were obtained from Benavente et al.[1] and values of maximum residue limits (MRLs) in milk samples were extracted from Comission Regulation (EU) No 37/2010[2].

**Sum of ciprofloxacin and enrofloxacin.

***Not for use in animals from which milk is produced for human consumption.

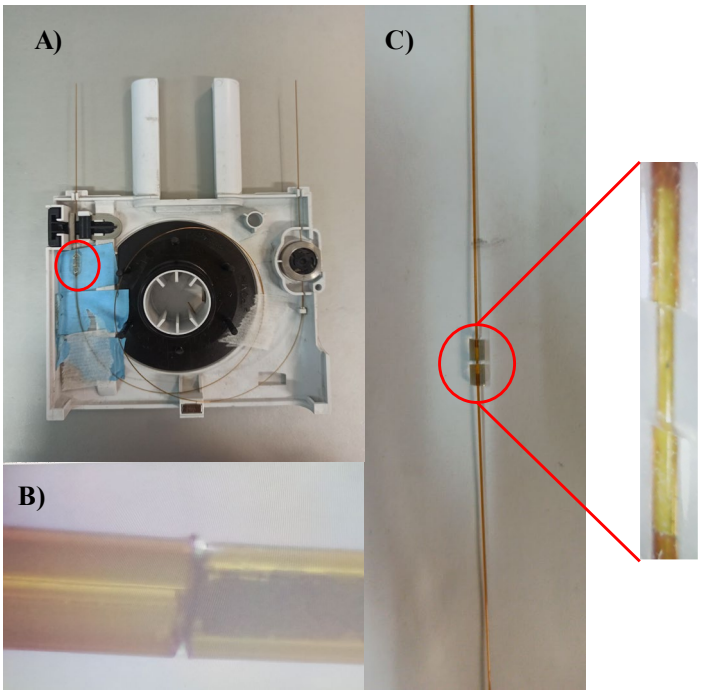

Fig. S1. Pictures of the SPE-CE-UV capillary with the microcartidge integrated near the inlet end. A) Installed in the commercial CE cartridge cassette (sealed with glue); B) connections between the microcartridge body and the separation capillary (80X, USB digital microscope) (before sealing with glue); and C) an example of a 4 mm microcartridge completely filled with HKUST-1@polymer sorbent (before sealing with glue).

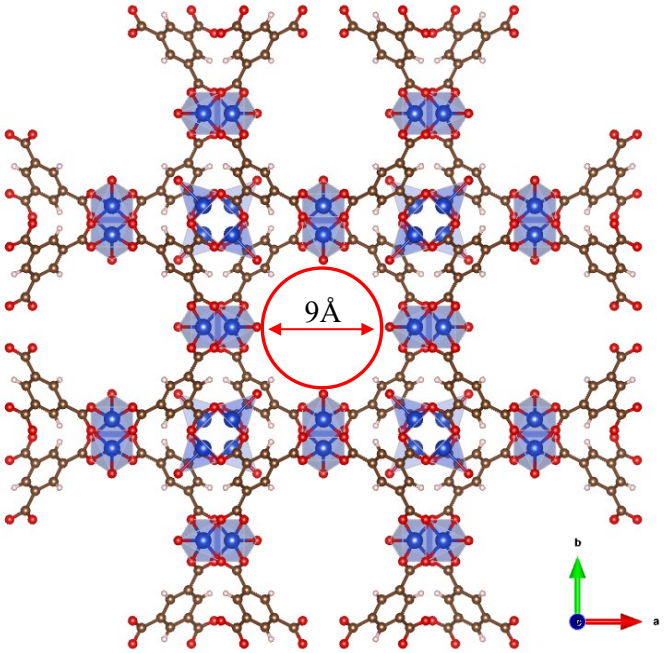

Fig. S2. Structure of HKUST-1with pore diameter [3]. Atom colors: Cu (blue), C (brown), H (pale pink) and O (red).

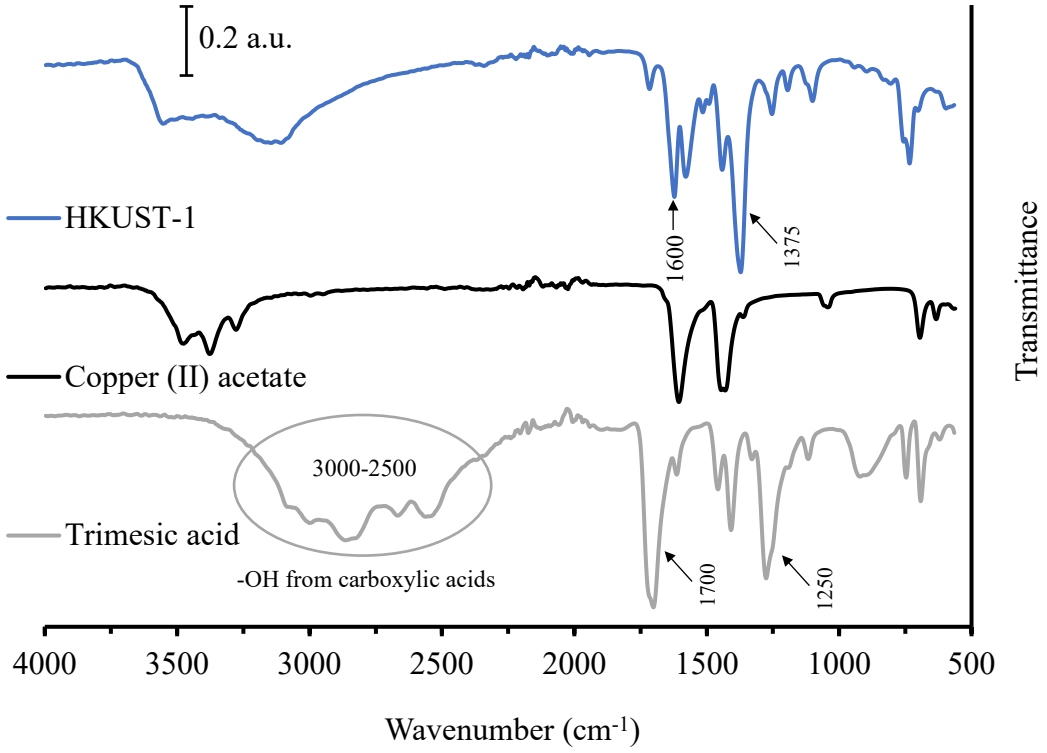

Fig. S3. FT-IR spectra of HKUST-1 precursors.

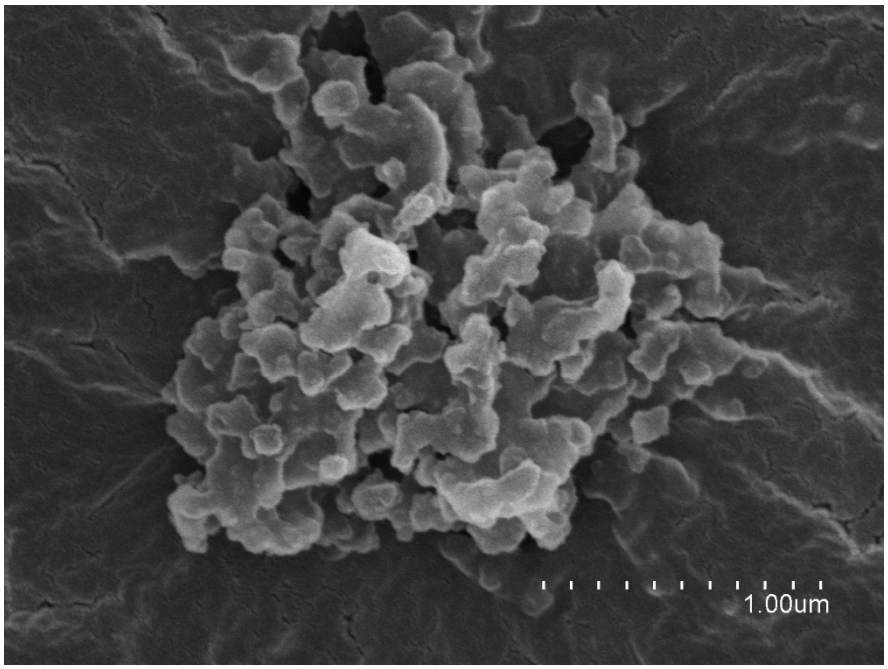

Fig. S4. SEM micrographs of the bare polymer.

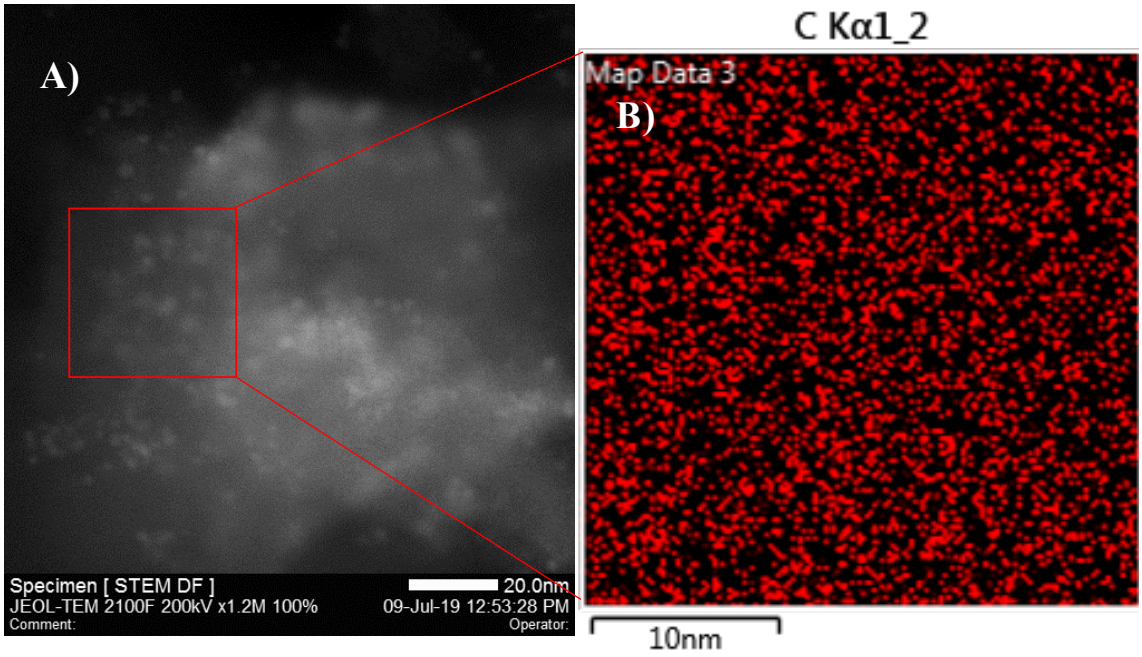

Fig. S5. A) STEM-HAADF micrograph and B) EDX elemental mapping analysis of the HKUST-1@polymer.

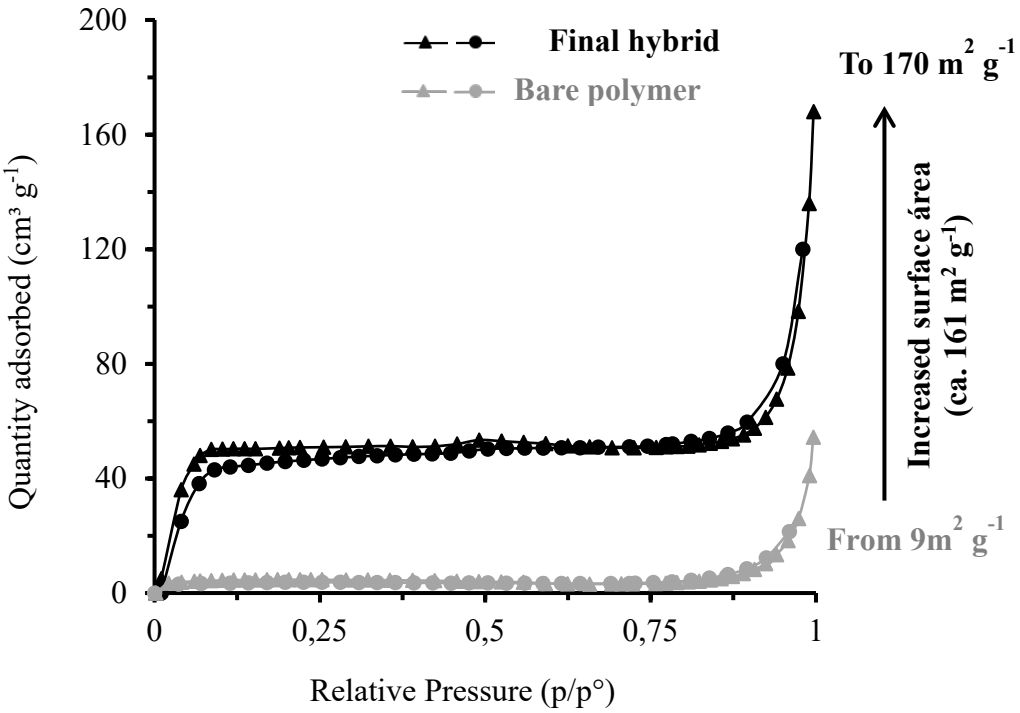

Fig. S6. Nitrogen adsorption and desorption isotherms at 77K for the hybrid material after four cycles and bare polymer without modification. Symbology: triangles are adsorption brand and circles indicate desorption brand, respectively.

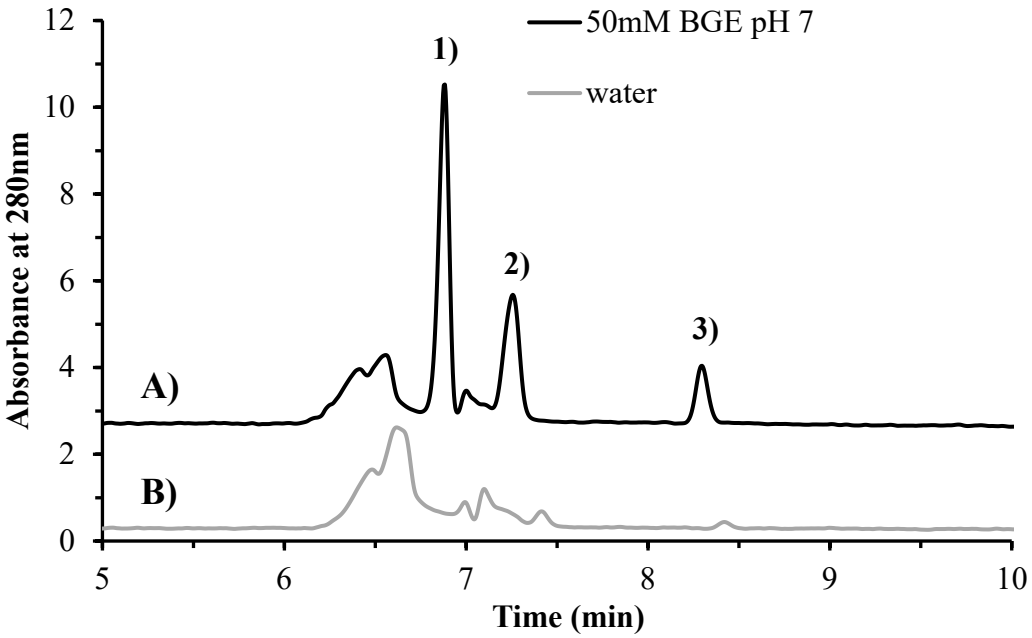

Fig. S7. SPE-CE-UV electropherograms (280 nm) for a 20 μg L^{-1} standard mixture of FQs loading the sample in A) BGE (50 mM phosphate buffer pH 7) and B) water. Peak identification: 1) DAN, 2) EFX and 3) DFX. The rest of experimental conditions (optimized method) are given in the experimental section.

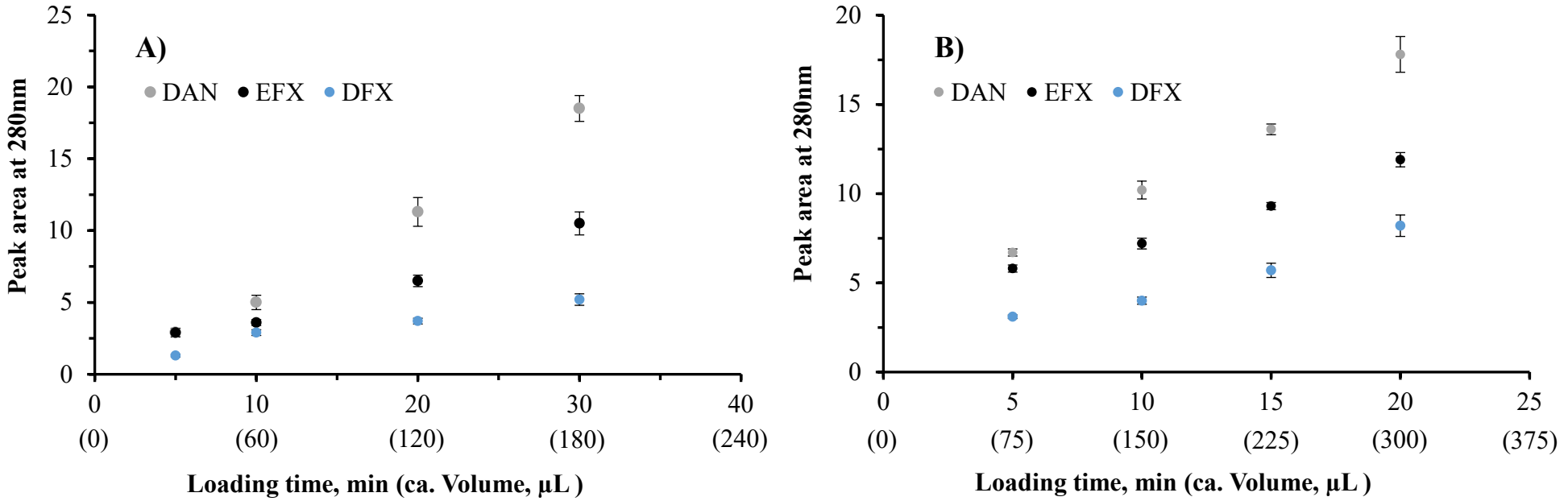

Fig. S8. Effect of the sample volume loaded on the peak areas with a 1 µg L^{-1} standard mixture of FQs at A) 930mbar and B) 2bar. The rest of experimental conditions (optimized method) are given in the experimental section (n = 3).

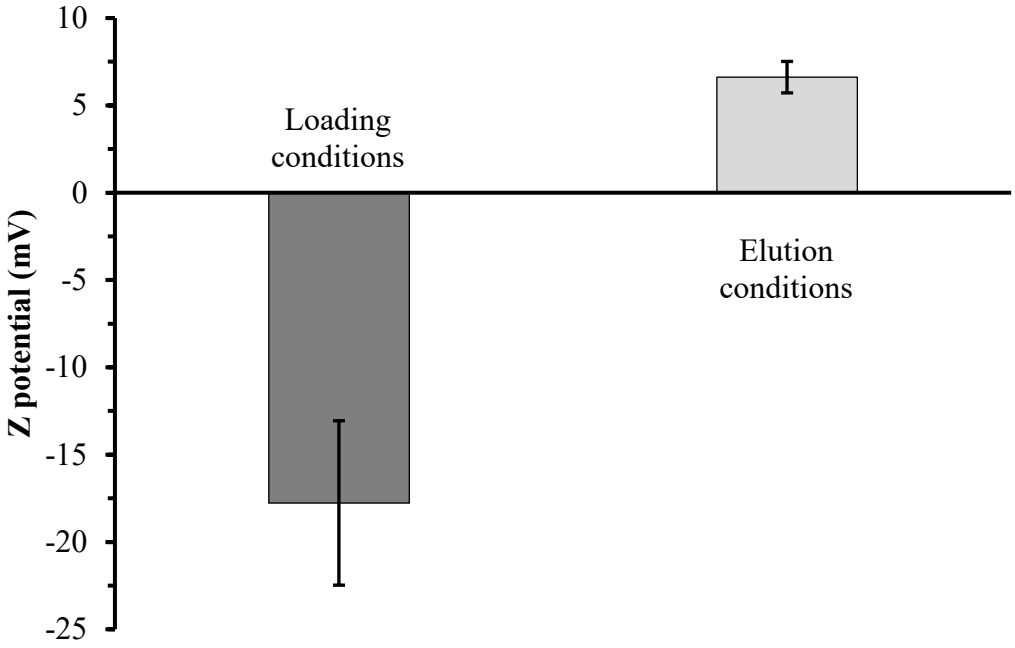

Fig. S9. Z potential analysis of the HKUST-1@polymer under the optimized conditions in SPE-CE-UV for A) loading (BGE, 50 mM phosphate pH 7) and B) elution (2% (v/v) FA in MeOH) conditions.

References

1. Benavente F, Giménez E, Barrón D, et al (2010) Modeling the electrophoretic behavior of quinolones in aqueous and hydroorganic media. Electrophoresis 31:965–972. https://doi.org/10.1002/elps.200900344

2. Barroso JM (2010) COMMISSION REGULATION (EU) No 37/2010 of 22 December 2009 on pharmacologically active substances and their classification regarding maximum residue limits in foodstuffs of animal origin. In: Official Journal of the European Union. pp 1–72

3. Mao Y, Li G, Guo Y, et al (2017) Foldable interpenetrated metal-organic frameworks/carbon nanotubes thin film for lithium-sulfur batteries. Nat Commun 8:14628. https://doi.org/10.1038/ncomms14628